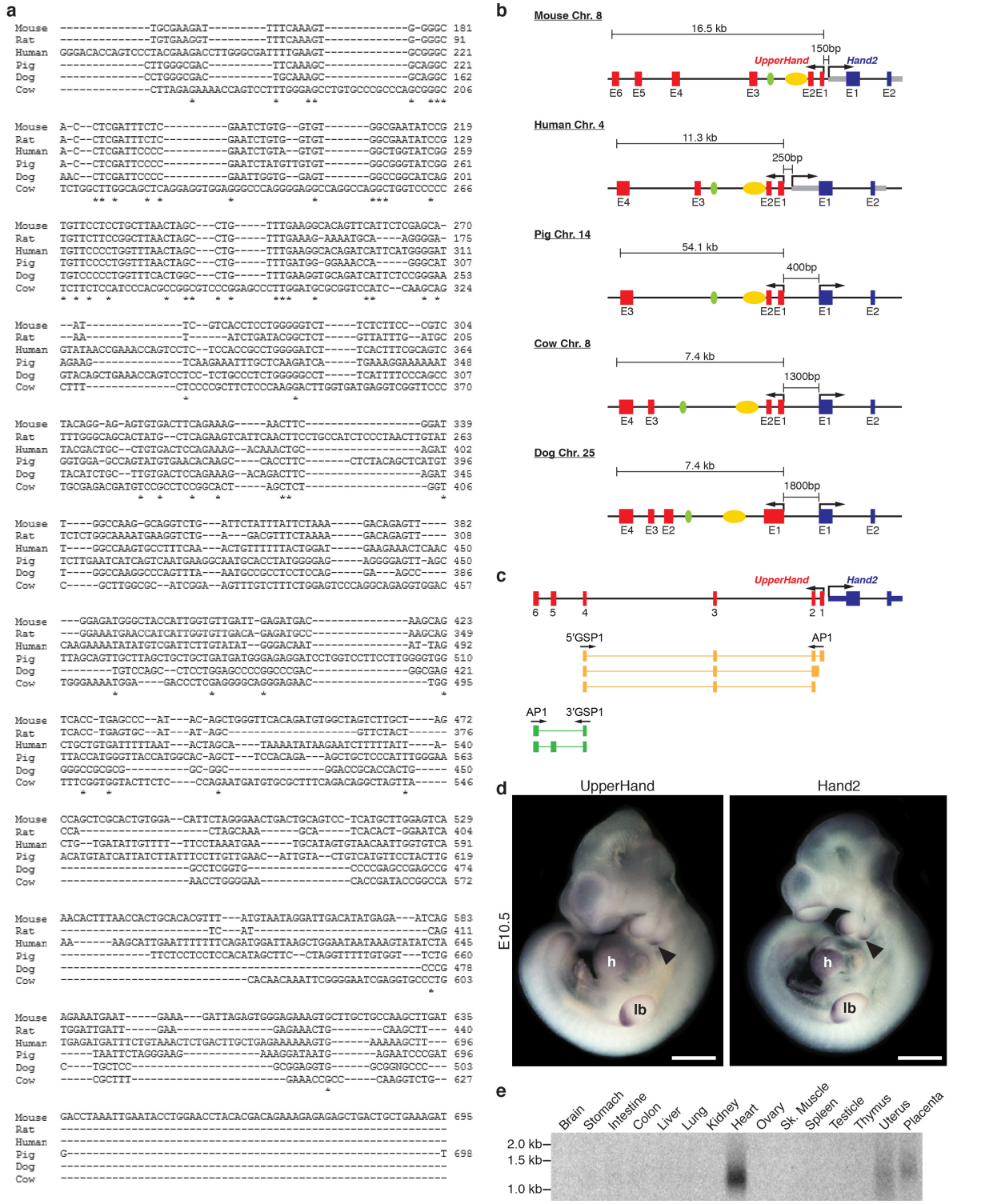

Extended Data Figure 1 | Sequence alignment of several mammalian *Uph* transcripts. a, Sequence alignment of several mammalian *Uph* transcripts performed using ClustalW. See Methods for source data. **b**, Diagram of the *Hand2* locus in mammals showing the genomic organization and orientation of *Uph*. The *Hand2* branchial arch enhancer (green) and cardiac enhancer (yellow) are shown. **c**, Diagram of the *Uph* transcripts expressed in the mouse heart, determined using 5′ and 3′ RACE using primers specific to exon 4 of *Uph*. AP1, marathon adaptor primer; 3′GSP, 3′ *Uph*-specific primer from exon 4; 5′GSP, 5′ *Uph*-specific primer from exon 4. **d**, Whole mount *in situ* hybridization of E10.5 mouse embryos. Expression was detected in heart, branchial arches (arrowhead), and limb bud. Scale bars, 1 mm. **e**, Northern blot analysis of total RNA from adult mouse tissues using a probe specific to the major *Uph* transcript. For gel source data, see Supplementary Fig. 1.

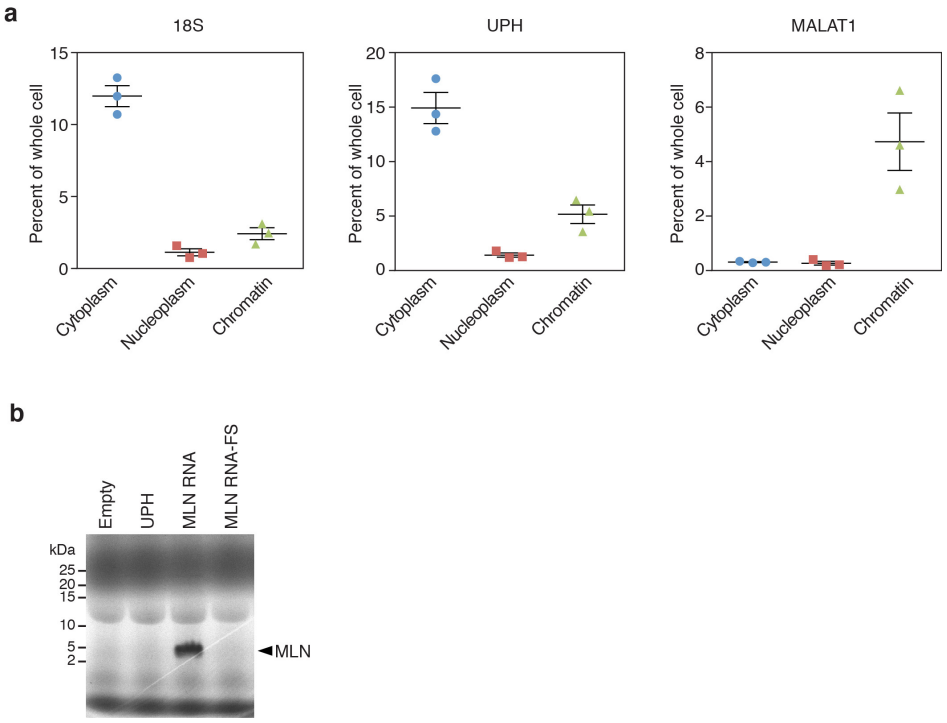

Extended Data Figure 2 | *Uph* is a cytoplasmic lncRNA. a, Subcellular fractionation of 18S, *Uph* and *Malat1* lncRNA in mouse neonatal cardiomyocytes ($n = 3$ biological replicates from 1 of 5 independent experiments; mean ± s.e.m.). **b**, *In vitro* transcription and translation of a plasmid encoding the major *Uph* RNA. A plasmid encoding the myoregulin (MLN) micropeptide was used as a positive control, and myoregulin with a frameshift mutation (MLN RNA-FS) was used as a negative control. In contrast to myoregulin, *Uph* and the negative control (MLN RNA-FS) did not produce any detectable proteins, indicating that *Uph* is a bona fide lncRNA. For gel source data, see Supplementary Fig. 1.

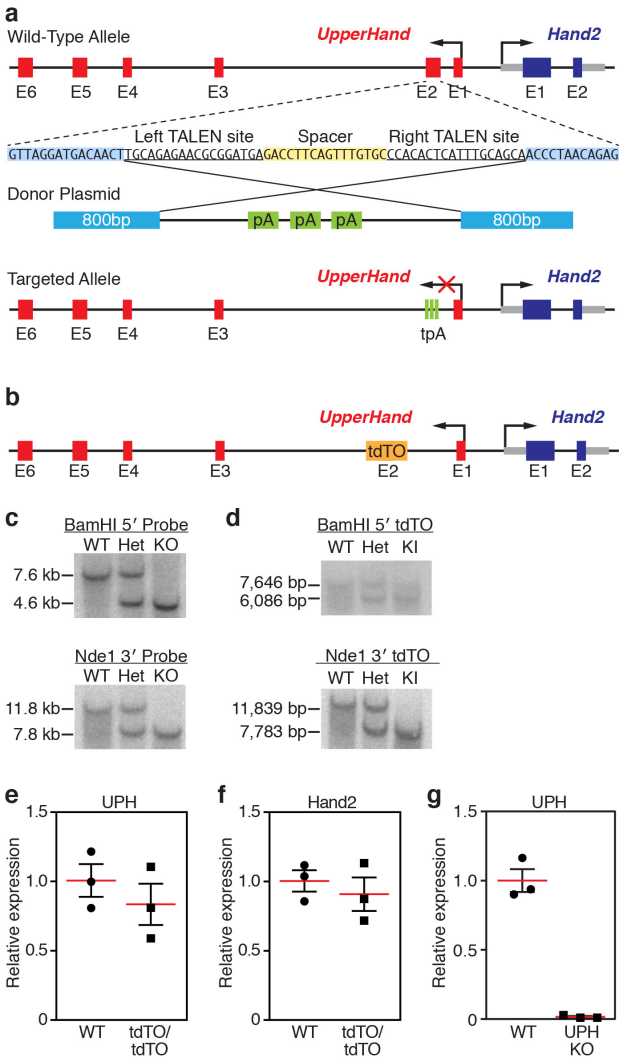

Extended Data Figure 3 | Targeting strategy for insertion of transcriptional termination or heterologous sequence into exon 2 of *Uph*. **a**, *Uph* KO targeting strategy. Transcription activator-like effector nucleases (TALENs) were used to insert a triple polyadenylation (tpA) termination sequence into exon 2 (E2) of *Uph*. **b**, Using the same TALEN pair as in **a**, we introduced the coding sequence of tdTO, lacking a polyadenylation sequence, into exon 2 of the *Uph* locus. Exon 2, which includes the tdTO coding sequence, was spliced out of the mature *Uph* transcript, preventing expression of tdTO in these mice. **c**, Southern blot analysis of wild-type, heterozygous $Uph^{+/-}$ (Het) and *Uph* KO genomic DNA. BamHI-digested DNA hybridized with a 5′-specific probe and NdeI-digested DNA hybridized with a 3′-specific probe. For gel source data, see Supplementary Fig. 1. **d**, Southern blot analysis of wild-type, $Uph^{tdTO/+}$ heterozygous and $Uph^{tdTO/tdTO}$ knock-in (KI) genomic DNA verified the correct targeting of the tdTO sequence into the *Uph* locus. DNA was digested with BamHI and hybridized with a 5′-specific probe or digested with NdeI and hybridized with a 3′-specific probe. For gel source data, see Supplementary Fig. 1. **e**, **f**, Expression of *Uph* (**e**) and *Hand2* (**f**) in wild-type and $Uph^{tdTO/tdTO}$ homozygous mice at E10.0 was not changed by the insertion of the tdTO sequence into exon 2 of the *Uph* locus ($n = 3$, representative of 3 independent experiments; mean ± s.e.m.). **g**, qPCR shows *Uph* transcripts decreased by ~97% in E10.5 hearts ($n = 3$ mice of each genotype from 1 of 3 independent experiments; mean ± s.e.m.).

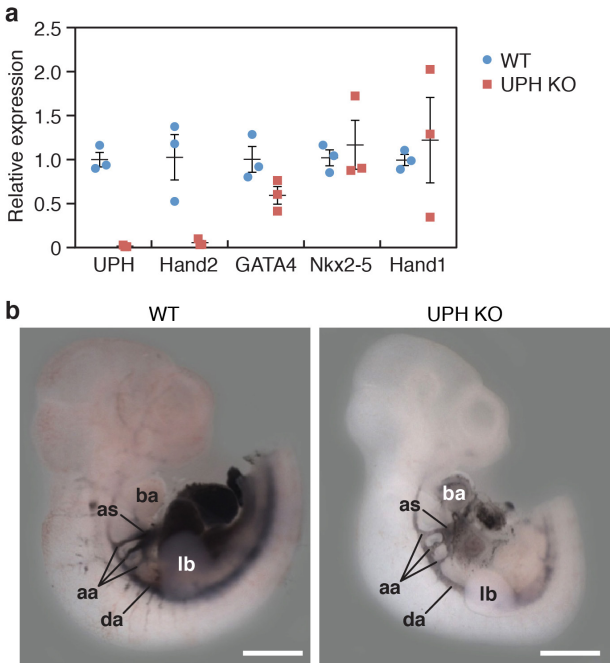

Extended Data Figure 4 | Aortic arch arteries are normal in *Uph* KO embryos. a, qPCR quantification of gene expression at E10.0 showed robust downregulation of *Uph* and *Hand2* expression in *Uph* KO hearts, with normal expression of other cardiac transcription factors ($n = 3$ mice of each genotype from 1 of 3 independent experiments; mean ± s.e.m.). **b**, India ink was injected into either the left ventricle of wild-type embryos or the single ventricle of *Uph* KO embryos at E10.5, to visualize the aortic arch arteries and circulation, which appeared normal in *Uph* KO embryos. aa, aortic arch arteries; as, aortic sac; da, dorsal aorta. Scale bars, 1 mm.

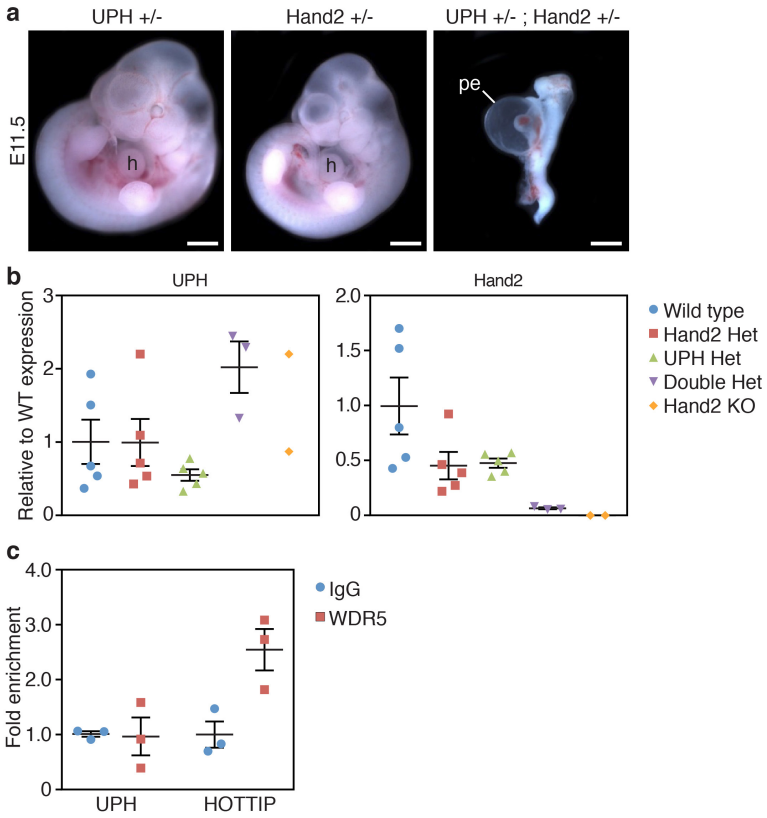

Extended Data Figure 5 | *Uph*$^{+/-}$ *Hand2*$^{+/-}$ compound heterozygotes recapitulate *Uph* KO phenotype. a, *Uph*$^{+/-}$ *Hand2*$^{+/-}$ double heterozygote embryos developed a single ventricle, pericardial effusion, and were severely growth restricted by E11.5. Scale bars, 1 mm. **b**, *Uph* expression is normal in double heterozygotes, whereas *Hand2* was reduced by ~90%, relative to wild-type embryos ($n = 5$ mice for wild type, *Hand2* het and *Uph* het, $n = 3$ for double het, $n = 2$ for *Hand2* KO, from 1 of 2 independent experiments; mean ± s.e.m.). **c**, Immunoprecipitation of RNA using either IgG or WDR5 in HL-1 cells followed by qPCR for *Uph* revealed no binding to WDR5. The WDR5-interacting lncRNA HOTTIP was used as a positive control ($n = 3$ biological replicates from 1 of 3 independent experiments; mean ± s.e.m.).

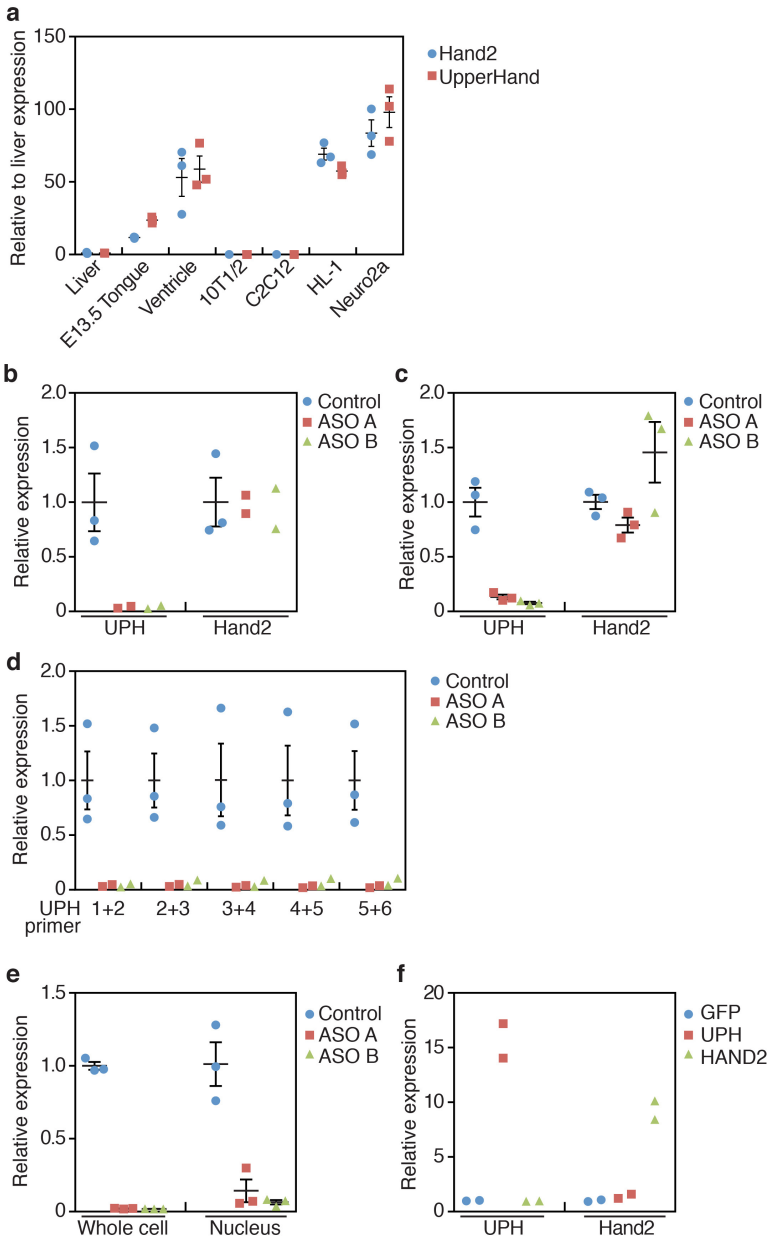

Extended Data Figure 6 | Knockdown of mature *Uph* transcripts in HL-1 or Neuro2a cells does not affect *Hand2* expression. a, Expression of *Uph* (red) and *Hand2* (blue) in various tissues and cell lines. *Uph* and *Hand2* are robustly expressed in the heart, and the HL-1 and Neuro2a cell lines. *Uph* and *Hand2* transcripts are not expressed in the liver, 10T1/2 fibroblasts or skeletal muscle C2C12 myotubes ($n = 3$ technical replicates; mean ± s.e.m.). **b**, **c**, *Uph* transcripts were reduced by ~90% in HL-1 (**b**) and Neuro2a (**c**) cells when transfected with two independent GapmeR antisense oligonucleotide probes (ASO A and B) against *Uph*. Expression of *Hand2* was not changed ($n = 2$ for ASO A and B, $n = 3$ for control, from 1 of 2 independent experiments; mean ± s.e.m.). **d**, *Uph* transcripts were similarly downregulated across each exon–exon junction, measured using qPCR ($n = 2$ for ASO A and B, $n = 3$ for control, from 1 of 2 independent experiments; mean ± s.e.m.). **e**, Fractionation of HL-1 cells transfected with control or *Uph*-specific ASOs. The nuclear fraction of antisense-oligonucleotide-treated HL-1 cells showed a similar downregulation of *Uph* transcripts ($n = 3$ biological replicates from 1 of 3 independent experiments; mean ± s.e.m.). **f**, Overexpression of enhanced green fluorescent protein (eGFP; blue), the major *Uph* RNA (red) or *Hand2* RNA (green) in HL-1 cells revealed that the mature *Uph* transcript did not alter *Hand2* expression relative to wild type, and that *Hand2* does not influence the expression of *Uph* in these cells ($n = 2$ biological replicates from 1 of 2 independent experiments; mean ± s.e.m.).

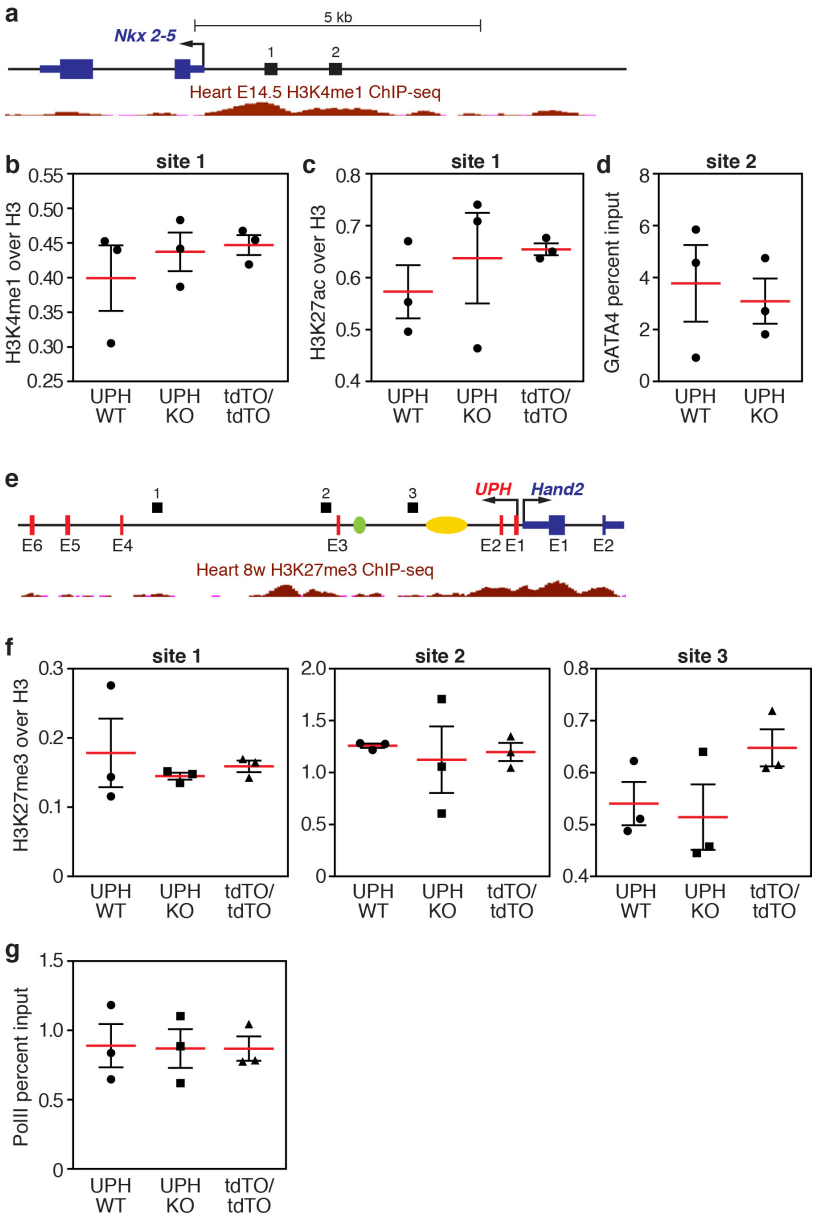

Extended Data Figure 7 | ChIP and qPCR analyses of active cardiac enhancers regulating *Nkx2-5* expression. a, Diagram of the *Nkx2-5* locus with numbers (1 and 2) indicating the region analysed by qPCR following ChIP. Shown in red are the ENCODE/LICR H3K4me1 active enhancer marks in the heart at E14.5. See Methods for source data. **b**, ChIP coupled with qPCR analysis of H3K4me1 marks, normalized to total histone H3, showed that the H3K4me1 marks bound to the *Nkx2-5* promoter region are unchanged between wild-type, *Uph* KO and $Uph^{tdTO/tdTO}$ homozygous hearts at E10.0. **c**, ChIP coupled with qPCR analysis of H3K27ac marks, normalized to total histone H3, showed that the H3K27ac marks bound to the *Nkx2-5* promoter region are unchanged between wild-type, *Uph* KO and $Uph^{tdTO/tdTO}$ homozygous hearts at E10.0. **d**, GATA4 binding to a GATA4 site in the *Nkx2-5* promoter is unchanged between wild-type and *Uph* KO hearts at E10.0. **e**, Diagram of the *Uph–Hand2* locus, with black bars indicating the regions analysed by qPCR following ChIP. Shown in red is the ENCODE/LICR H3K27me3 track for mouse heart. See Methods for source data. The branchial arch enhancer (green) and cardiac enhancer (yellow) are shown. **f**, ChIP coupled with qPCR analysis of the polycomb repressive marker H3K27me3, normalized to total histone H3, showed no differences between genotypes at each locus (1–3) indicated in the diagram in **e**. **g**, qPCR revealed no difference in the levels of Ser2-phosphorylated RNAPII between genotypes at the *Nkx2-5* gene body. Each point is one of 3 technical replicates of 5 pooled hearts for each genotype in each ChIP experiment, from 1 of 2 independent experiments; mean ± s.e.m.

Extended Data Table 1 | Relevant sequences

SEQUENCE NAME	FORWARD	REVERSE
Full Length UPH sequence	CACTCATAACCATAAGATAATTAAAACGG	TTTAAAAAATAATTTTTAATATACTATGTGCATGGTTGGATAGGT
UPH qPCR primers	CATTCTCGAGCAATTCGTCA	TGGTAGCCCATCTCCAACTC
UPH ISH probe	GATGAGACCTTCAGTTTGTGCC	ATACTATGTGCATGGTTGGATAGGT
Hand2 ISH probe	ATGAGTCTGGTGGGGGGC	TCACTGCTTGAGCTCCAGG
UPH targeting 5'arm	TATCGGAGCTCGCACCTCGGAGCTGGGAA	GATACGCGGCCGCGGATCCAGTTGTCATCCTAACTTGGGTCA
UPH targeting 3'arm	TATCGGCTAGCCATATGACCCTAACAGAGATTGCGAAGA	GATACATCGATCAGGGCAGTTAGGTCTCAGC
UPH 5' WT genotyping	CTCCTCTCCGGACAAGAATC	TGCTGCAAATGAGTGTGG
UPH 5' KO genotyping	CTCCTCTCCGGACAAGAATC	GGTTCCGGATCCACTAGTTCT
UPH 3' WT genotyping	AGAGAACGCGGATGAGACCT	CCCTTGCAAACAGAAGAAAGG
UPH 3' KO genotyping	GACCTGCAGCCCAAGCTA	CCCTTGCAAACAGAAGAAAGG
tdTO 5' WT genotyping	CTCCTCTCCGGACAAGAATC	TGCTGCAAATGAGTGTGG
tdTO 5' KO genotyping	CTCCTCTCCGGACAAGAATC	ATGACCTCCTCGCCCTTG
tdTO 3' WT genotyping	AGAGAACGCGGATGAGACCT	CCCTTGCAAACAGAAGAAAGG
tdTO 3' KO genotyping	GACCTGCAGCCCAAGCTA	CCCTTGCAAACAGAAGAAAGG
Southern BamHI probe	TGGTTTTCTTGTCGTTGCTG	CTGACTGGGTCCTTGAGCAT
Southern NdeI probe	TCCTGGGAAGGCACTATGTC	ACCTTCTCCTGCCCTTCATT
Hand1 ISH probe	CCATCATCACCACTCACACC	GCGCCCTTTAATCCTCTTCT
Nkx2-5 ISH probe	TATGGCTACAACGCCTACCC	GTGTGGAATCCGTCGAAAGT
ASO negative control	AACACGTCTATACGC	
ASO UPH A	GCTAGTTAAGCAGGA	
ASO UPH B	ATTCAATTTAGGTCAT	
5GSP1		CAGCTGTATGGGCTCAGGTGACTGC
3GSP1		TGGAGATGGGCTACCATTGGTGTTGA
AP1	CCATCCTAATACGACTCACTATAGGGC	
Hand2 - Gata site	TTTACCCACTGGTCCCCTCT	TGGACAACATGGGACAGAAA
Nkx2-5 - Gata site	CTGCAACTATCACCCGGAAT	AGAAACCCCCATCTGTTTCC
UPH ChIP site 1	TCACCTCCCCATGTCTTTTC	GAGGAACCTGCATTGCTTTC
UPH ChIP site 2	ACCTCGGGCTTTCGATCTTA	GCTTGGGAAGGTAAGCCTTT
UPH ChIP site 3	GAAACTAGCCTTGCCCCTTC	GGGTGCCTAGGGAGGAATAC
Nkx2-5 ChIP - site 1	ACTGTGAAGCCCAATTCCAG	AACCAGAAATTGTGGCAAGG